Supporting Information

Fabrication of Arbitrary-Shaped and Nitrogen-Doped Graphene Aerogel for Highly Compressible All Solid-State Supercapacitors

Degang Jiang [†a], Chenwei Li [†a], Wenrong Yang [b], Jizhen Zhang [b], Jingquan Liu*[a]

[a] College of Materials Science and Engineering, Institute for Graphene Applied Technology Innovation, Qingdao University, Ningxia Road 308 Qingdao 266071, P. R. China.

E-mail: jliu@qdu.edu.cn (Jingquan Liu)

[b] School of Life and Environmental Sciences, Deakin University, Melbourne VIC 3217, Australia

[†] Degang Jiang and Chenwei Li contributed equally to this work.

Characterizations

TEM image was obtained using a JEM-2100F electron microscope with an accelerating voltage of 200 kV. The morphology of the as-prepared samples was investigated by JEOL 6701 field-emission scanning electron microscope (JEOL 6701, Japan), with energy dispersive X-ray spectroscopy to investigate the morphology and structure of the samples. The XPS spectra of as-prepared samples were examined on a PerkineElmer PHI-5702 multifunctional X-ray photoelectron spectroscope (XPS, Physical Electronics, USA). The structures of the as-prepared samples were analyzed with XRD (DX2700, China) at a scan rate (2θ) of 2^{o} min^{-1} ranging from 5^{o} to 80^{o}, operating at Cu Kα radiation (l=1.5418 Å) with an accelerating voltage of 40 kV and an applied current of 30 mA. The compressive tests were performed with a rheometer (ARES-G2, TA Instruments, USA) in the axial-compression testing mode at a strain rate of 100% strain min^{-1}, and all the graphene aerogel samples were tested at room temperature. All the electrochemical tests were performed using a CHI 760E electrochemical workstation.

Calculations

The specific capacitances of the GASC were calculated from their GCDs which were carried out on symmetrical supercapacitor systems according to the following equation:

$$C = \frac{2I\Delta t}{m\Delta V} \quad (1)$$

Where C is the specific capacitance (F g^{-1}), I is the discharge current (A), Δt is the discharge time (s), m (g) is the mass of single GA electrode and ΔV is the voltage window (V).

The energy density and power density of symmetrical supercapacitor systems were calculated using the following equations:

$$E = \frac{C_t \Delta V^2}{2 \times 3.6} \quad (2)$$

$$P = \frac{E}{t} \quad (3)$$

Where E (Wh kg^{-1}) is the energy density, P (W kg^{-1}) is the power density of the symmetrical GASC system, C_t (F g^{-1}) is the specific capacitance of the whole symmetrical GASC system, which is equal to C/2. ΔV (V) is the voltage window, and t (h) is the discharge time, respectively.

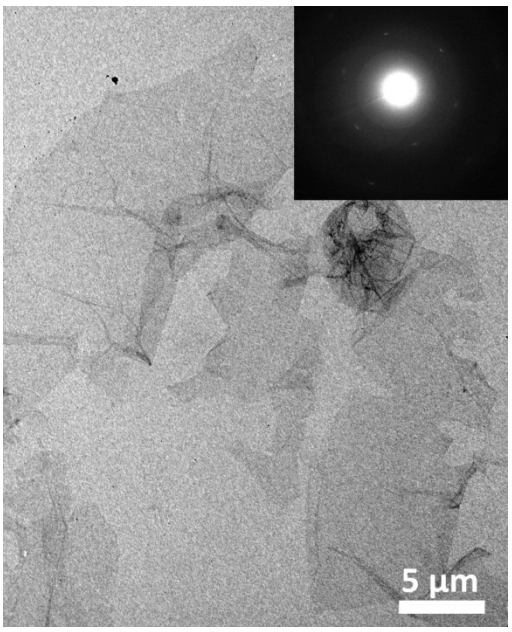

Figure S1. TEM image of graphene oxide (GO). The inset is the selected-area electron diffraction (SAED) pattern.

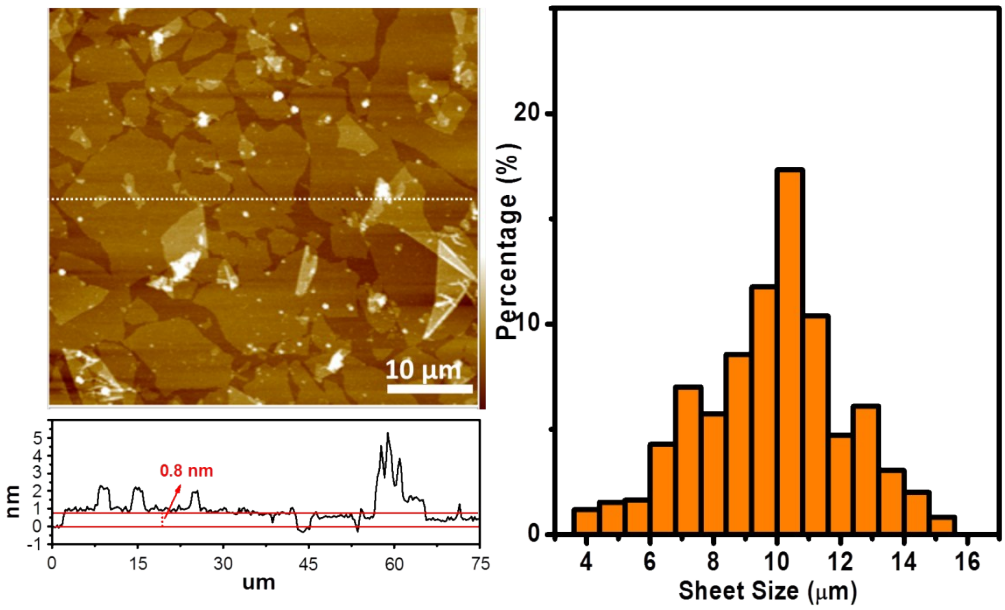

Figure S2. AFM image of graphene oxide (GO) and the sheet size distribution.

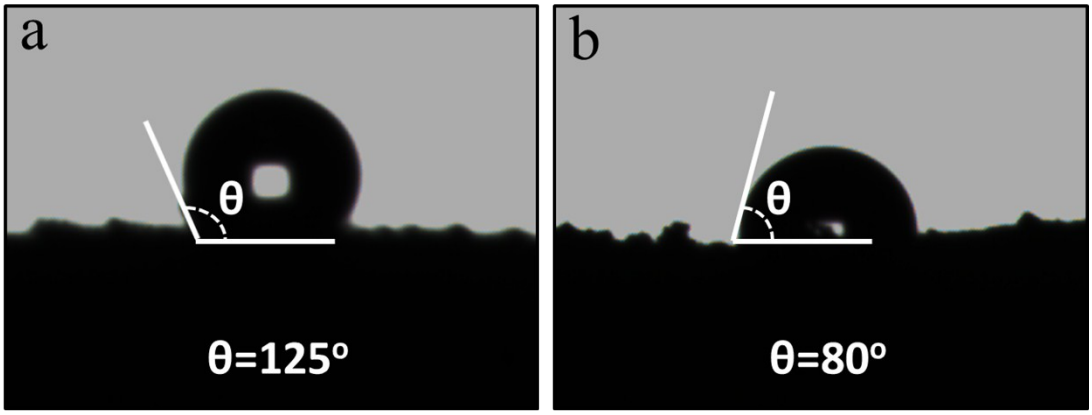

Figure S3. The water contact angle measurement for a) GMF, b) the nitrogen-doped GA.

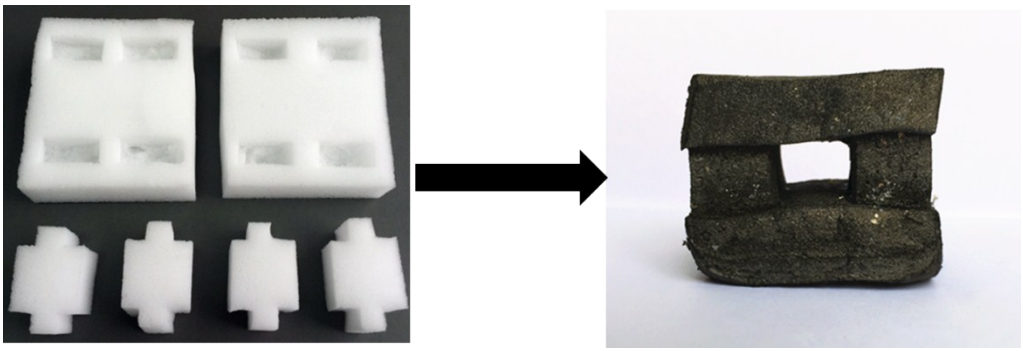

Figure S4. The fabrication of 3-D structured GA cube from special designed MF components.

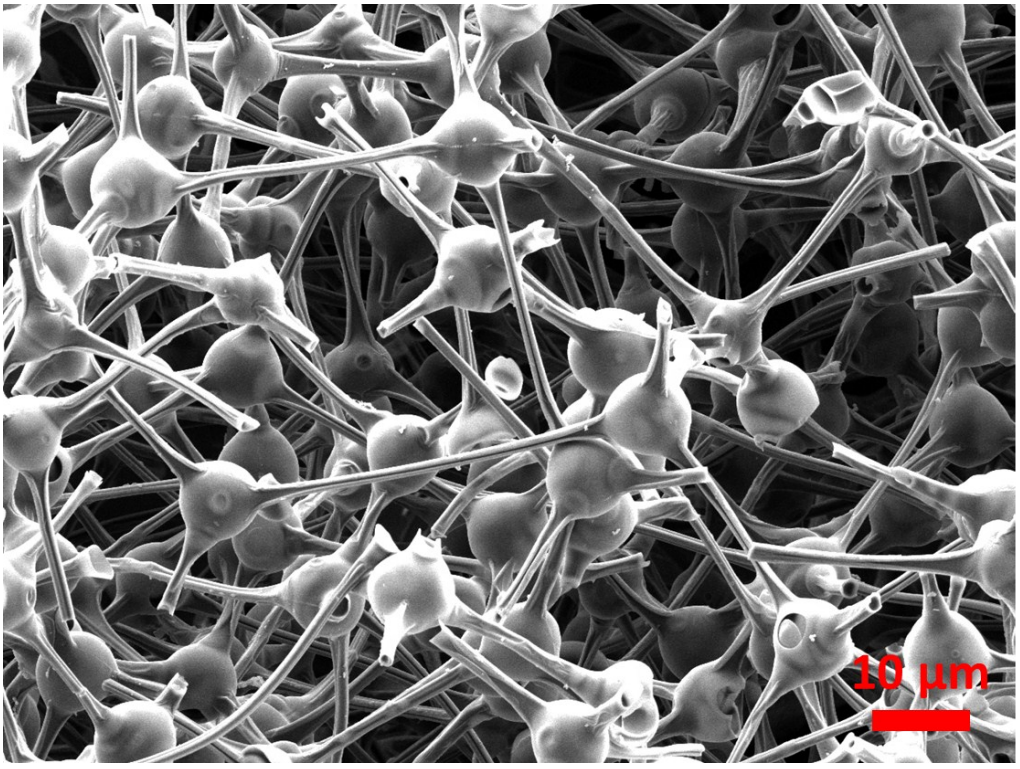

Figure S5. SEM image of the carbonized MF (CMF).

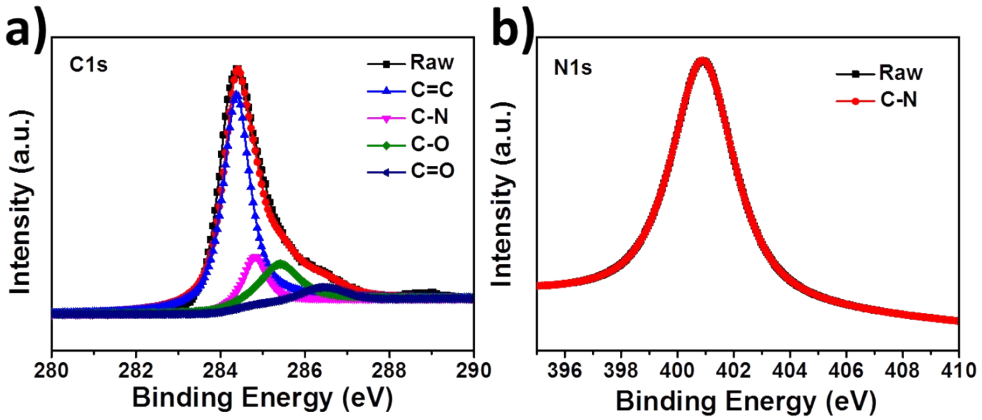

c)

Element	Atomic ratio (%)
C1s	86.61
N1s	1.82
O1s	9.99

Figure S6. XPS spectra for a) C1s, b) N1s of nitrogen-doped GA. c) The atomic ratio of C, N and O in GA.

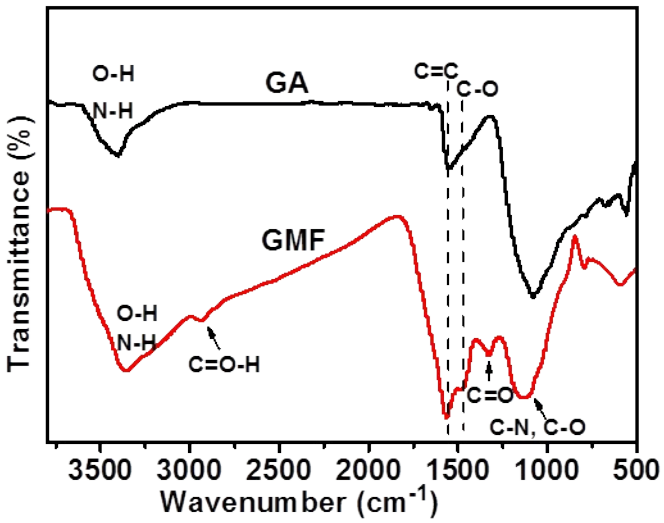

Figure S7. FTIR transmittance spectra of GMF and GA.

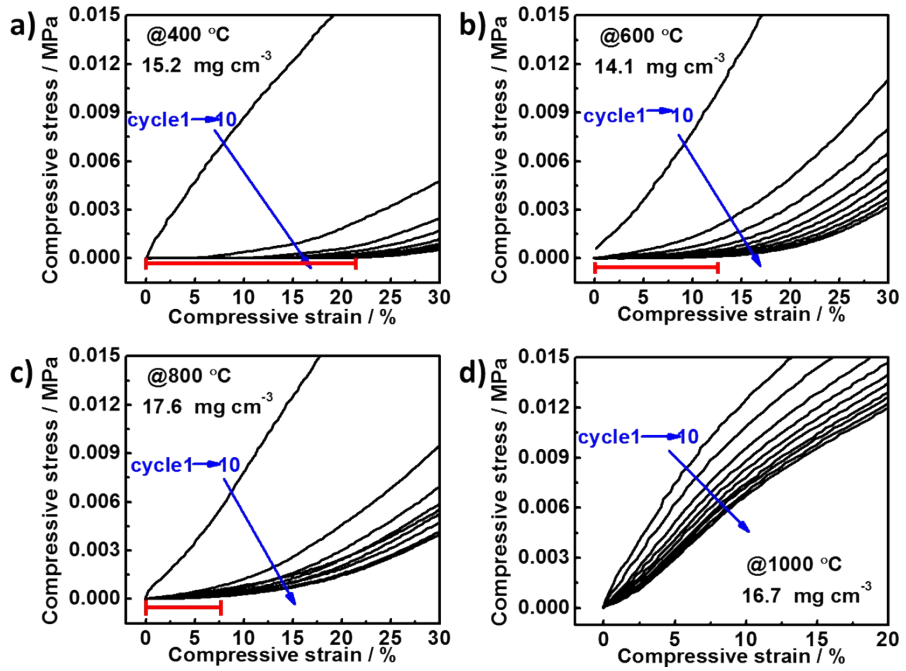

Figure S8. Cyclic compressive stress-strain curves under the strain of 80% (the enlarged images at low stress area) of GA annealed at different temperature : (a) at 400 °C; (b) at 600 °C; (c) at 800 °C and (d) at 1000 °C.

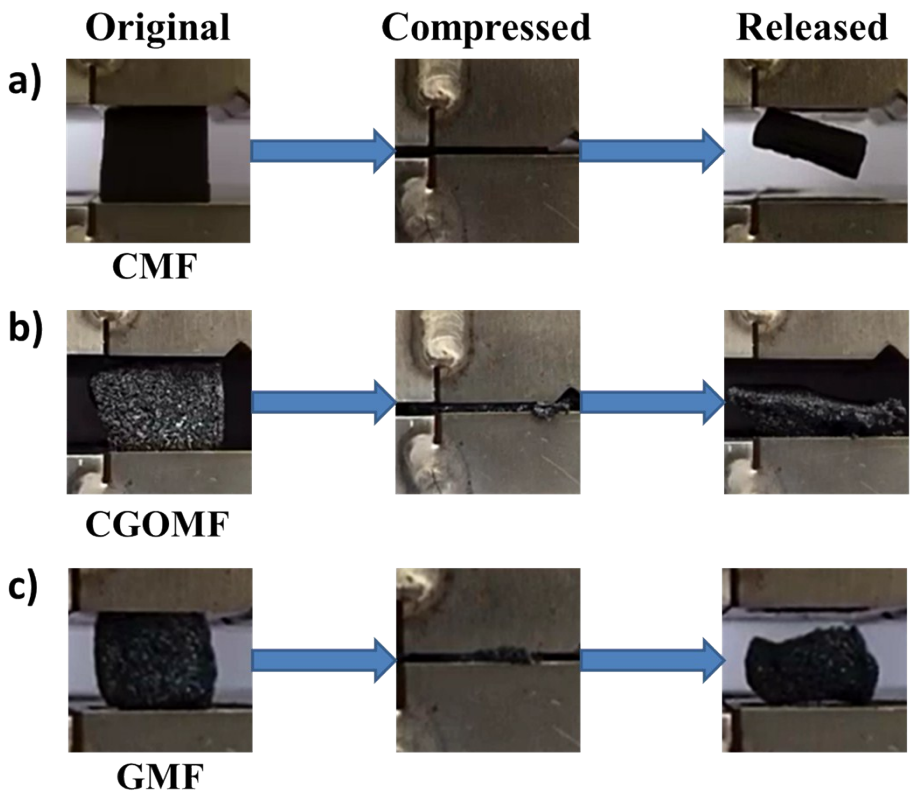

Figure S9. The digital images showing compressibility of CMF, CGOMF, and GMF, respectively.

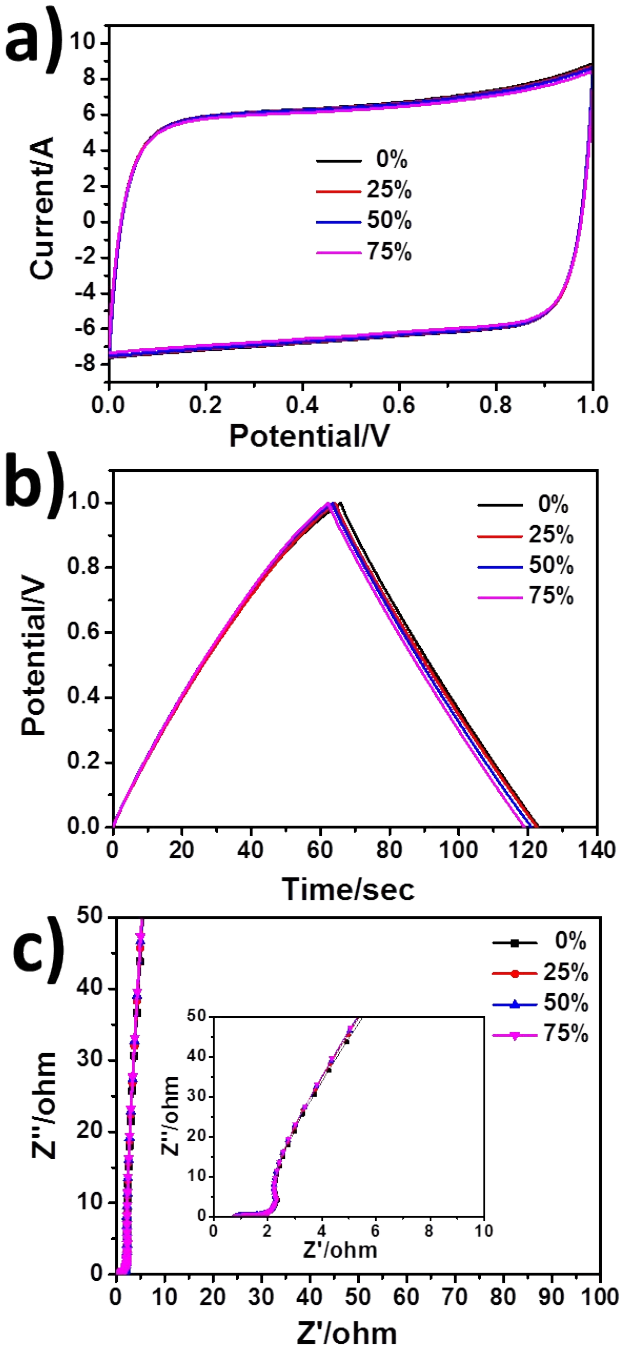

Figure S10. a) The CV curves, b) galvanostatic charge-discharge curves and c) Nyquist plots of GASC under different compressible strains.

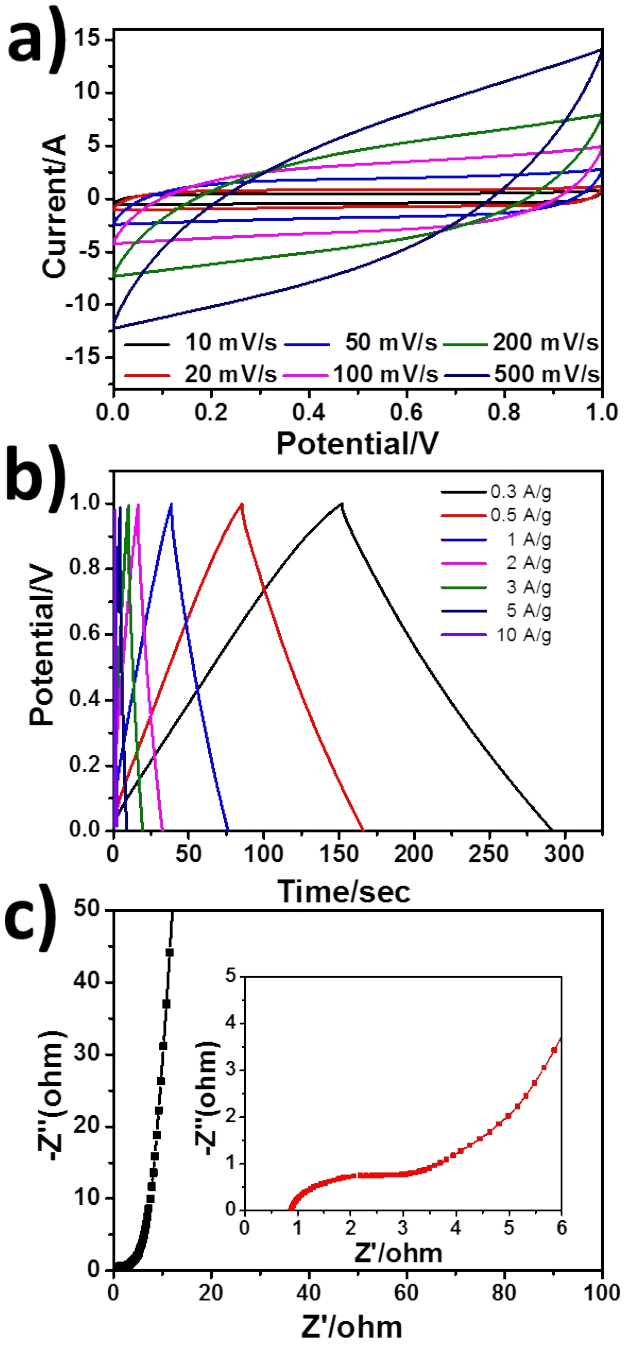

Figure S11. a) The CV curves, b) galvanostatic charge-discharge curves and c) Nyquist plots of CMF electrodes.

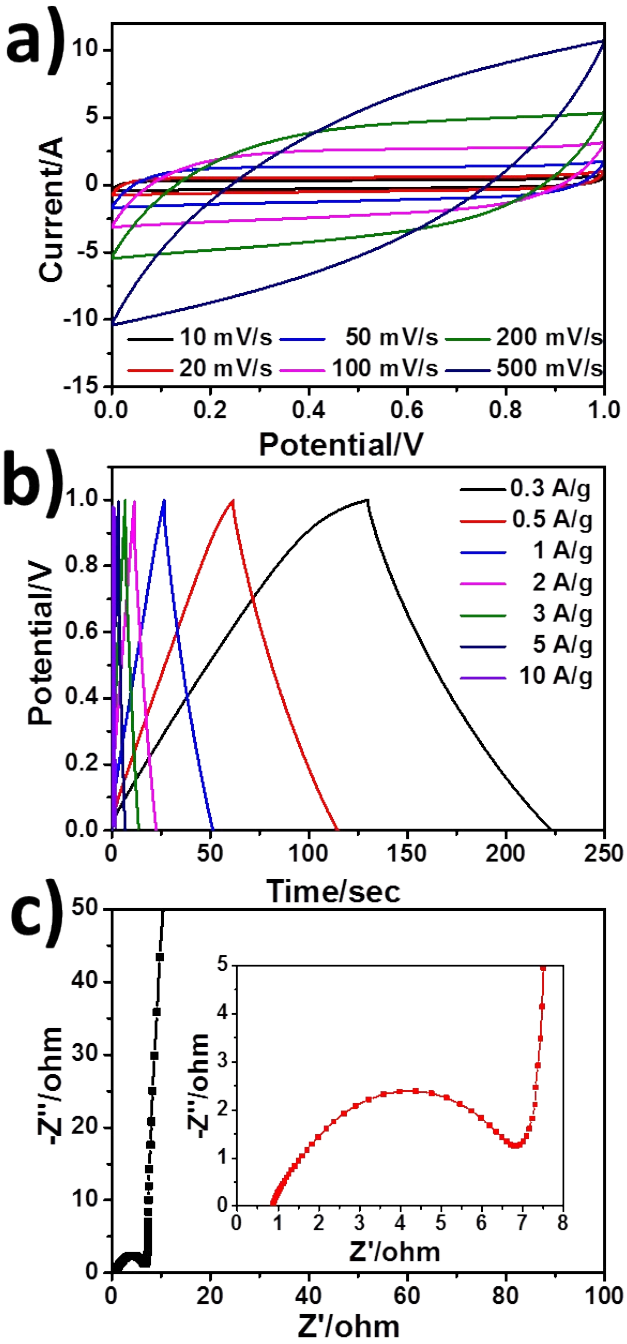

Figure S12. a) The CV curves, b) galvanostatic charge-discharge curves and c) Nyquist plots of GMF electrodes.

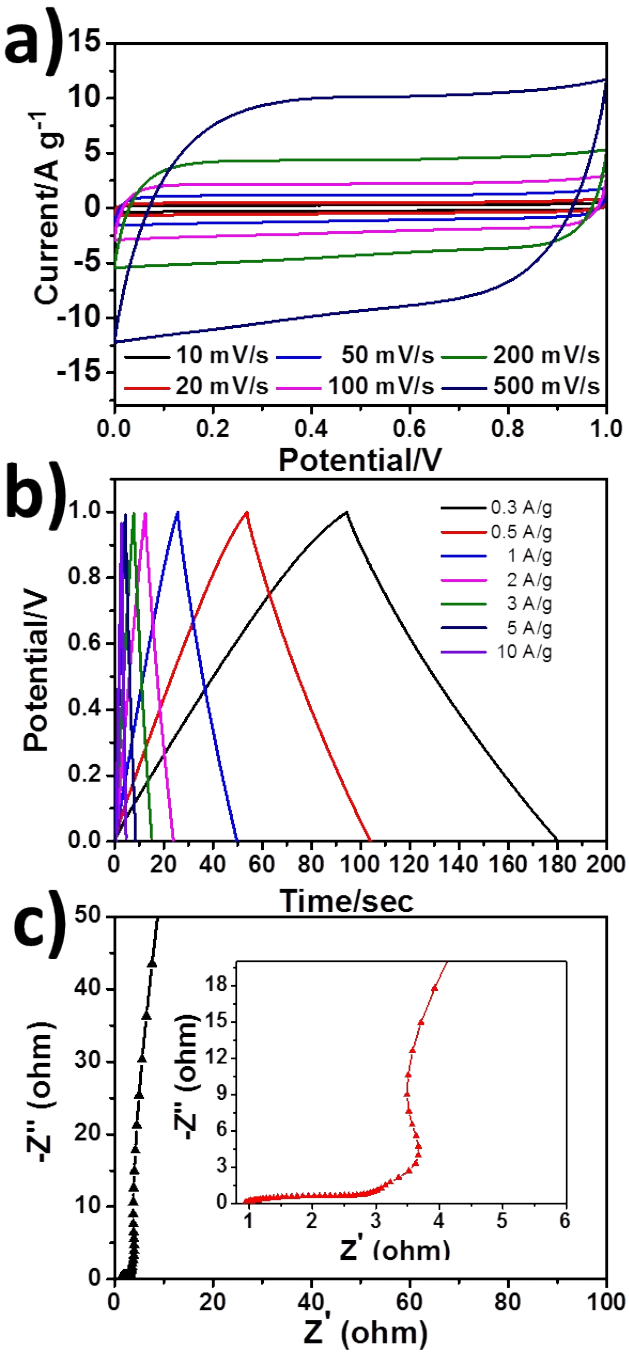

Figure S13. a) The CV curves, b) galvanostatic charge-discharge curves and c) Nyquist plots of CGOMF electrodes.

(a)

Sample	CMF	GMF	CGOMF	GA
Conductivity (S m^{-1})	8.5	2.1	3.0	67.2

(b)

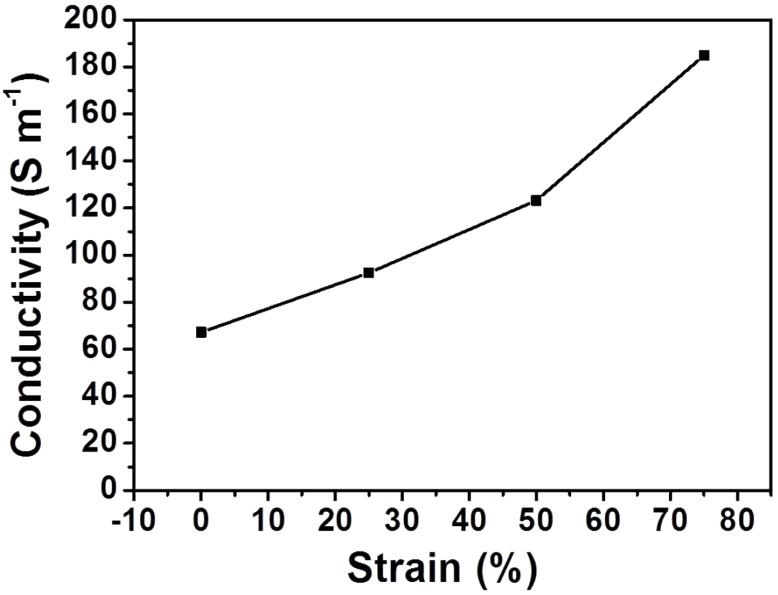

Figure S14. (a) The conductivity of CMF, GMF, CGOMF and GA. (b) The conductivity of GA under different compressible strains.

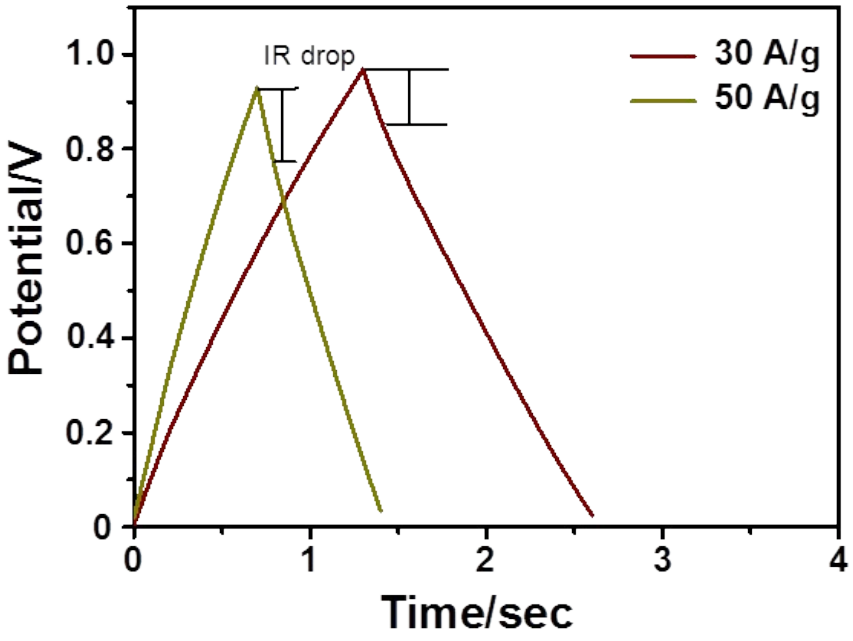

Figure S15. The charge-discharge curves of GA electrodes at 30 and 50 A g^{-1}.

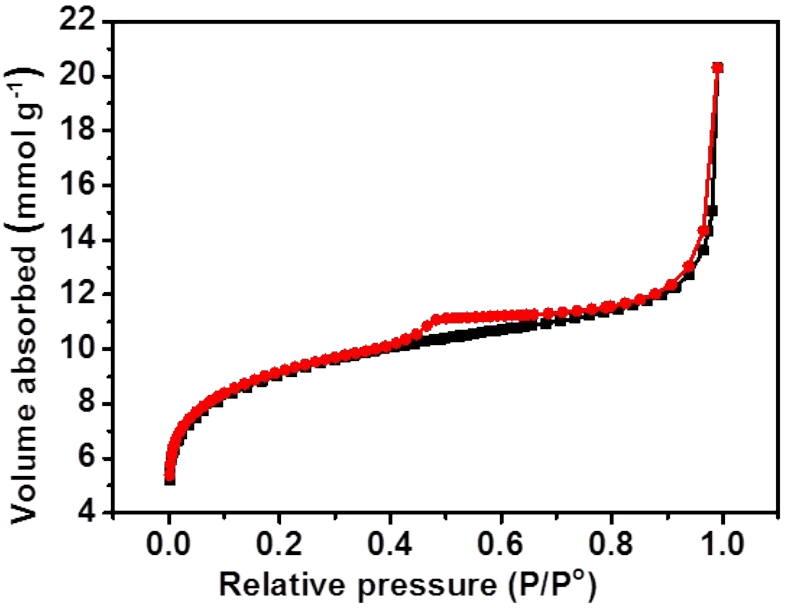

Figure S16. The N_2 adsorption-desorption isotherms of GA.

Table S1. Specific capacitance values and maximum compression obtained with various electrode materials

Electrode	Specific Capacitance ($F\ g^{-1}$)	Maximum Compression (%)	Ref
Graphene aerogel	150	90	This work
CNC-MWCNT-PPy	45.6	80	1
CNT-graphene	103	50	2
CNT-graphene-ppy	225	50	2
CNF aerogel	25	75	3
Graphene-CNT	70	90	4
PANI-SWCNT sponge	216	60	5
Graphene aerogel	144	70	6
CNT sponge	10.1	60	7
CNT-PPy	255.4	60	7
CNT sponge	29.3	50	8
CNT-MnO_2	183.7	50	8
Graphene-PPy	220	80	9
Macro/Mesoporous CNT sponge	143	60	10
Carbon foam	52	60	11
GNR-PU	87.5	80	12
RGO aerogel	110	60	13
CNT sponge	80.2	70	14

Reference

1. K. Y. Shi, X. Yang, E. D. Cranston and I. Zhitomirsky, *Adv. Funct. Mater.*, 2016, **26**, 6437-6445.

2. Y. Zhang, Z. Zhen, Z. Zhang, J. Lao, J. Wei, K. Wang, F. Kang and H. Zhu, *Electrochim. Acta*, 2015, **157**, 134-141.

3. G. Nystrom, A. Marais, E. Karabulut, L. Wagberg, Y. Cui and M. M. Hamedi, *Nat. Commun.*, 2015, **6**.

4. E. Wilson and M. F. Islam, *Acs Applied Materials & Interfaces*, 2015, **7**, 5612-5618.

5. Z. Q. Niu, W. Y. Zhou, X. D. Chen, J. Chen and S. S. Xie, *Adv. Mater.*, 2015, **27**, 6002-6008.

6. S. Ye and J. Feng, *Acs Applied Materials & Interfaces*, 2014, **6**, 9671-9679.

7. P. Li, E. Shi, Y. Yang, Y. Shang, Q. Peng, S. Wu, J. Wei, K. Wang, H. Zhu, Q. Yuan, A. Cao and D. Wu, *Nano Res.*, 2014, **7**, 209-218.

8. P. Li, Y. Yang, E. Shi, Q. Shen, Y. Shang, S. Wu, J. Wei, K. Wang, H. Zhu, Q. Yuan, A. Cao and D. Wu, *Acs Applied Materials & Interfaces*, 2014, **6**, 5228-5234.

9. Y. Zhao, J. Liu, Y. Hu, H. Cheng, C. Hu, C. Jiang, L. Jiang, A. Cao and L. Qu, *Adv. Mater.*, 2013, **25**, 591-595.
10. Y. B. Yang, P. X. Li, S. T. Wu, X. Y. Li, E. Z. Shi, Q. C. Shen, D. H. Wu, W. J. Xu, A. Y. Cao and Q. Yuan, *Chem.-Eur. J.*, 2015, **21**, 6157-6164.
11. K. Xiao, L. X. Ding, G. X. Liu, H. B. Chen, S. Q. Wang and H. H. Wang, *Adv. Mater.*, 2016, **28**, 5997.
12. Y. J. Ding, J. Q. Zhu, C. H. Wang, B. Dai, Y. X. Li, Y. Y. Qin, F. Xu, Q. Y. Peng, Z. Z. Yang, J. Bai, W. X. Cao, Y. Yuan and Y. B. Li, *Carbon*, 2016, **104**, 133-140.
13. J.-Y. Hong, B. M. Bak, J. J. Wie, J. Kong and H. S. Park, *Adv. Funct. Mater.*, 2015, **25**, 1053-1062.
14. X. Cheng, X. Gui, Z. Lin, Y. Zheng, M. Liu, R. Zhan, Y. Zhu and Z. Tang, *J. Mater. Chem. A*, 2015, **3**, 20927-20934.